McDonald, J. K., & Schwabe, C. (1977) in *Proteinases in Mammalian Cells and Tissues* (Barrett, A. J., Ed.) pp 311-386, Elsevier/North-Holland Biomedical Press, Amsterdam.
Neurath, H., & Walsh, K. A. (1976) *Proc. Natl. Acad. Sci. U.S.A. 73*, 3825-3832.
Peterson, L. M., Sokolovsky, M., & Vallee, B. L. (1976) *Biochemistry 15*, 2501.
Peterson, L. M., Holmquist, B., & Bethune, J. L. (1982) *Anal. Biochem. 125*, 420.
Petra, P. H. (1970) *Methods Enzymol. 19*, 460-503.
Robbins, K. C., & Summaria, L. (1970) *Methods Enzymol. 19*, 184-199.
Rosen, F. S., Alper, C. A., Pensky, J., Klemperer, M. R., & Donaldson, V. H. (1971) *J. Clin. Invest. 50*, 2143.
Stenflo, J., Fernlund, P., Egan, W., & Roepstorff, P. (1974) *Proc. Natl. Acad. Sci. U.S.A. 71*, 2730.
Walsh, K. A. (1970) *Methods Enzymol. 19*, 41-63.
Yamasaki, M., Brown, J. R., Cox, D. J., Greenshields, R. N., Wade, R. D., & Neurath, H. (1963) *Biochemistry 2*, 859.
Zimmerman, T. S., Ratnoff, O. D., & Powell, A. E. (1971) *J. Clin. Invest. 50*, 244.

Rotational Diffusion of *Escherichia coli* RNA Polymerase Free and Bound to Deoxyribonucleic Acid in Nonspecific Complexes†

R. H. Austin,‡ Joanne Karohl,§ and Thomas M. Jovin*

ABSTRACT: We have studied the rotational diffusion of *Escherichia coli* RNA polymerase free in solution and bound nonspecifically to DNA fragments. The rotational motion was measured by the decay in anisotropy of the triplet–triplet absorption by using as probes either the liganded enzyme inhibitor Rose Bengal or eosin 5′-isothiocyanate conjugated to the protein. The time resolution extended from 10 ns to 1 ms. Free RNA polymerase (holoenzyme) at high salt concentration (1 M NaCl) is monomeric and diffuses at 5 °C with a rotational correlation time of 0.66 μs, corresponding to an equivalent hydrodynamic sphere with a radius of 7.4 nm. These values and the known molecular weight are most compatible with a nonspherical shape, e.g., an oblate ellipsoid with an axial ratio of about 3. In 0.1 M NaCl, the holoenzyme is dimeric and has a rotational correlation time of 2 μs. The decay of anisotropy is at least biexponential upon binding RNA polymerase to calf thymus DNA or to poly[d(A-T)]. The fast component with half of the amplitude has decay kinetics comparable to those seen with the free monomeric enzyme. The slow component has a rotational correlation time of about 14 μs and is independent of DNA chain length in the range >180 base pairs. Both rotational correlation times decrease with temperature, and the relative amplitudes change such that the faster component dominates at higher temperature. The rotational relaxation of the enzyme–DNA complexes is discussed in terms of alternative models involving rigid rod–sphere diffusion, conformational changes in the enzyme and/or DNA, sliding motions of the protein along the DNA, and torsional-bending motions of DNA envisioned as a deformable rod.

The transcription of DNA is effected through a sequence of reactions involving different modes of interaction between RNA polymerase and its double-helical template:

(a) Formation of the prerecognition complex: The enzyme binds nonspecifically to a region of the DNA by an outside purely electrostatic mechanism leading to the release of counterions from the DNA (Shaner et al., 1983). These binary complexes have been visualized by electron microscopy (Williams, 1977; Kadesch et al., 1980) and characterized thermodynamically by chromatographic (de Haseth et al., 1978), sedimentation (Lohman et al., 1980; Revzin & Woychik, 1981), and nitrocellulose filter binding (Melançon et al., 1982) techniques.

(b) Nonspecific translocation: The enzyme migrates on the DNA by a random-walk process which probably involves one of or a combination of various mechanisms (Berg et al., 1981; Barkley, 1981; Berg & Ehrenberg, 1982; Fried & Crothers, 1983): "sliding", a one-dimensional diffusion; "hopping", a series of spatially correlated microscopic dissociations and reassociations; and "intradomain transfer", direct transfer of the protein from one segment of a randomly coiled (i.e., long) DNA molecule to another.

(c) Promoter recognition: RNA polymerase encounters and rapidly identifies a promoter sequence either by interactions of complementary matrices of hydrogen-bond donors and acceptors (von Hippel & Bear, 1983) and/or by recognition of specific sequence-imposed patterns of twist angles (Kabsch et al., 1982); conformational changes and associated protonation reactions of the enzyme are involved (Strauss et al., 1980). The contact region extends over about 30 base pairs upstream starting near position −10 (relative to the initiation site) and is restricted primarily to one side of the double helix (Siebenlist et al., 1980).

(d) Promoter activation and (e) transcription (initiation, elongation–translocation, termination): These processes will not be considered further here.

The purpose of our investigation was to probe by direct physical techniques the dynamic properties of the protein and DNA partners in the binary and ternary complexes described above. We have restricted ourselves initially to the nonspecific interactions, step a above. The method of transient absorption

† From the Abteilung Molekulare Biologie, Max Planck Institut für Biophysikalische Chemie, D-3400 Gottingen, FRG. *Received June 3, 1982; revised manuscript received March 9, 1983.*
‡ Present address: Department of Physics, Princeton University, Princeton, NJ 08544.
§ Present address: Department of Biochemistry, Carnegie-Mellon University, Pittsburgh, PA 15213.

0006-2960/83/0422-3082$01.50/0

dichroism using long-lived triplet probes (Cherry, 1978) was used to measure the rotational diffusion properties of the system in the time domain of 10 ns–10 ms. Time-resolved fluorescence depolarization has been applied extensively to assess the rotational motions and thus shape, size, flexibility, and environmental characteristics of molecules in solution (Rigler & Ehrenberg, 1973). However, RNA nucleotidyltransferase (RNAP)[1] and DNA are too large for accurate measurements on the time scale of fluorescent techniques. Long-lived (0.1–10 ms) triplet probes provide the spectroscopic means for observing global rotations while the intense pulsed laser beam and high-speed electronics enable the resolution of faster local segmental relaxations.

The RNA polymerase (holoenzyme) from *Escherichia coli* (EC 2.7.7.6; RNAP) is an oligomer of five subunits ($\alpha_2\beta\beta'$)σ with an aggregate molecular mass of 490 kdalton. Its physicochemical properties are extremely well documented (Burgess, 1976; Levine et al., 1980; Kumar, 1981). Subunit σ plays an essential role in promoter recognition but is shed shortly after initiation, yielding the core enzyme which completes the extension of the RNA product. Two triplet probes reacting with the enzyme were used, Rose Bengal (RB) and eosin 5′-isothiocyanate (EITC). Rose Bengal binds stoichiometrically to *Escherichia coli* RNA polymerase and acts as an inhibitor of elongation but not of template binding (Wu, C.-W., & Wu, 1973). EITC reacts nonspecifically with primary amines of the numerous lysine side chains (Cherry et al., 1976).

The DNA used in most of the measurements was the synthetic polynucleotide poly[d(A-T)] which mimics many of the properties of natural promoters. It has been estimated that the binding site for this polymer extends over 28–60 bp, 10–17 of which are locally denatured by each polymerase molecule (Williams, 1977; Melnikova et al., 1978; Reisbig et al., 1979; Shimamoto & Wu, 1980). The DNA helix appears to be stabilized outside the locus of unwinding (Reisbig et al., 1981). Upon binding, the holoenzyme loses some secondary (Levine et al., 1980) and possibly higher order (Stender, 1979) structure and also monomerizes from the predominantly dimeric form in free solution (Krakow & von der Helm, 1970). It has been postulated that an RNAP molecule may possess more than one binding site for DNA (Reisbig et al., 1981; Park et al., 1980). Poly[d(A-T)] is a good template for in vitro RNA synthesis with a very short lag time in its approach to a steady-state initiation rate (McClure, 1980) and a relatively high affinity for the enzyme at elevated ionic strength (0.25–0.4 M NaCl; Revzin & Woychik, 1981).

Materials and Methods

RNAP. RNAP was purified from mid-phase *E. coli* cells (Merck, Darmstadt) by using the procedure of Burgess (1976). The enzyme was assayed according to Berg et al. (1971) with bacteriophage T7 DNA template. Three RNAP preparations were used. The first was a gift of Dr. G. Rhodes and consisted of 80–100% holoenzyme according to polyacrylamide gel electrophoresis analysis of the subunits. The specific activity was 7000 units/mg. The second preparation was core RNAP, i.e., was devoid of σ subunit. The third enzyme sample was identical with the first in every respect except it contained a contaminating protein which resisted attempts at further purification. However, the contaminant was not labeled with EITC in our procedure, and the observed patterns of anisotropy decay were identical with those of preparation 1.

Reagents. Rose Bengal was the product of Fluka, Germany, and was used without further purification. Eosin 5′-isothiocyanate was obtained from Molecular Probes, Inc. (Junction City, OR). High molecular weight calf thymus DNA was from Worthington. Poly[d(A-T)] was synthesized with *E. coli* DNA polymerase I and deproteinized by extraction with 1 M NaCl and 0.2% lauryl sulfate. The preparation was fractionated in a preparative 5–20% sucrose density gradient containing 1 M NaCl. Individual fractions were characterized by analytical velocity sedimentation under neutral and denaturing (alkaline) conditions according to Studier (1965). Chain lengths in base pairs were calculated from the data at neutral pH. The standard buffer designated TEGD was 10 mM Tris-HCl, pH 7.5, 5% (v/v) glycerol, 0.1 mM EDTA, and 0.1 mM dithiothreitol.

Labeling of RNAP with EITC. Reaction at low temperature according to the following protocol led to the greatest retention of enzymatic activity. Stoichiometric amounts of enzyme and EITC (about 20 μM) were incubated at −20 °C for 2 days in 0.1 M sodium carbonate buffer, pH 9, and 50% glycerol. (The reaction was essentially quantitative according to absorption criteria after 7 days.) Unreacted dye was removed by chromatography with Sephadex G-25 equilibrated with TEGD. The retention of enzymatic activity was greater than 95%. Polyacrylamide gel electrophoretic analysis demonstrated that the predominant labeling with eosin was of the β, β', and σ subunits, with less than 10% of the fluorescence associated with the α subunits.

Transient Dichroism Measurements. A nitrogen laser (Lambda Physik Model M1000; Gottingen, West Germany) pumped a dye laser to provide the excitation pulse to the sample. The output from the dye laser was a 0.5-mJ pulse at 500 nm, was approximately 5 ns in duration, and was vertically polarized to greater than 90%.

The monitoring light was a He–Ne laser (Spectra Physics 120) with a 100% polarized beam and 5-mW power. The plane of polarization of the laser was rotated 45° to the vertical so that equal components of horizontal and vertical polarization impinged on the sample. Two front-surface aluminum mirrors formed an optical cavity so that the monitoring beam passed 5 times through the sample volume, effectively giving a 5-fold increase in optical depth. The sample volume required was only 50 μL. The laser beam passed through the sample was directed through a 632.8-nm (1-nm bandwidth) interference filter (Oriel Optics) and a RG600 glass filter (Schott, Mainz) to remove any stray photolysis light or fluorescence. After the optical filters, a polarizing beam splitter (Halle, Berlin) split the beam into the orthogonal vertical and horizontal components.

The two beams emerging from the polarizing beam splitter entered separate photomultipliers (RCA 1P28A/V1). A 100-Ω resistor on the anode converted the current to a voltage which was subsequently amplified by two 20-dB high-speed amplifiers (Lecroy Electronics VV100) for each channel. The direct current (dc)-coupled output voltages were monitored continuously during a run by two digital voltmeters driven by a low-pass amplifier. This allowed adjustment and matching of the dc gains so that good anisotropy nulls resulted for free dye. The two signals were directed to a high-speed differential amplifier (Optical Electronics, Tucson) with a 50-dB common-mode rejection ratio at 100 MHz and captured by a Biomation 8100 transient recorder. The digitized trace was transferred to a Fabri-Tek 1074 signal averager and summed. The dye laser was run at 20 Hz, and typically 4096 shots were

[1] Abbreviations: RNAP, RNA nucleotidyltransferase; RB, Rose Bengal; EITC, eosin 5′-isothiocyanate; TEGD, standard Tris buffer; Tris, tris(hydroxymethyl)aminomethane; bp, base pair(s); EDTA, ethylenediaminetetraacetic acid.

stored per curve. Extensive signal averaging was necessary due to the laser beam mode noise: 10 mV root mean square out of 1.00-V dc and with a 100-MHz bandwidth. With 5 μM RB in the RNAP–DNA experiments, the single-shot signal to noise ratio was 0.1.

The sample cuvette was a 10 mm × 2 mm quartz cell with all sides polished. Removal of oxygen from the sample was of crucial importance since oxygen quenches the triplet at close to the diffusion-limited rate. Argon of 99.995% purity (Messer Griesheim, Kassel) was passed through an Oxysorb oxygen removal filter (Messer Grisheim) to remove trace oxygen and then over the sample surface in the cuvette while a small magnetic stirring bar rotated at 1 Hz so as to slowly exchange the gas with the liquid. Even with prolonged stirring, we were unable to reproduce the literature value of 1.5 ms for the eosin triplet lifetime [see Austin et al. (1979) for examples of EITC triplet lifetimes at low concentrations], but instead obtained a value of 146 μs. We attribute this finding to singlet–triplet quenching occurring at the high concentrations of the dye in solution (5–10 μM). The reduced lifetime should not have influenced the anisotropy decay curves appreciably since the rotational correlation times were still considerably shorter.

Excitation with the polarized actinic beam produces a photoselected partially ordered population of triplet-state molecules. The initial dichroism of the triplet–triplet absorption signals decays due to Brownian motion. The protocol for acquisition of the time-resolved data was as follows: the system averaged the parallel polarization signal ($\Delta I_\parallel$) for N sweeps with subsequent storage on magnetic tape, followed by the same procedure for the difference signal ($\Delta I = \Delta I_\parallel - \Delta I_\perp$). This method removed common mode noise from laser fluctuations in the monitoring beam. The decay curves were synthesized from the following combined records:

$$S(t) = \Delta I_\parallel + 2\Delta I_\perp = 3\Delta I_\parallel - 2\Delta I \quad (1a)$$

$$r(t) = \Delta I/[S(t)] \quad (1b)$$

$S(t)$ provides a measure of the total triplet signal, and the anisotropy $r(t)$ represents the rotational depolarization. The decay curves were analyzed by a nonlinear multiexponential least-squares program. The time constants constitute the triplet lifetime(s) (τ) and the rotational correlation time(s) (ϕ) in the case of $S(t)$ and $r(t)$, respectively. The error bars discussed under Results were not derived from the fitting routine but represent the standard deviations from a number (usually five) of identical experiments. [For additional details of triplet-state spectroscopy and the use of polarized emission, see Austin et al. (1979) and Jovin et al. (1981).]

Data Analysis. The rotational relaxation of the triplet probes conjugated to RNA polymerase in free solution and complexed to DNA was analyzed according to the formalism for a rigid hydrated sphere [$r(t) \equiv r_s(t)$] and for a rigid ellipsoid of revolution [$r(t) \equiv r_e(t)$; Rigler & Ehrenberg, 1973].

$$r_s(t) = r_{in}e^{-t/\phi} = r_0 r' e^{-t/\phi} \quad (2)$$

$$r_e(t) = r'\sum_{i=1}^{3}\alpha_i e^{-t/\phi_i} \qquad r_0 = \sum\alpha_i \quad (3)$$

The observed initial anisotropy (r_{in}) is given by the product of the photoselection factor (r_0) and a depolarization term (r') which includes the combined effects of local probe motion and segmental mobility in the time domain faster than that experimentally resolved ($<\sim 100$ ns).

$$r_0 = (2/5)P_2(\cos\delta) \quad (4)$$

$P_2(x) = (3x^2 - 1)/2$ is the second Legendre polynomial, and δ is the angle between the singlet–singlet and triplet–triplet absorption transition moments corresponding to the actinic and monitoring processes.

For the sphere, the rotational correlation time ϕ depends upon the temperature T, viscosity η, and hydrated molecular volume V_h.

$$\phi = 1/(6D_s) \qquad D_s = kT/(V_h\eta) \quad (5)$$

$$V_h = (\bar{v} + \Gamma'\bar{v}_s)M_r/N \qquad r_h = [3V_h/(4\pi)]^{1/3} \quad (6)$$

D_s is the rotational diffusion constant, k is Boltzmann's constant, M_r is the molecular weight and r_h the radius of the hydrated protein (treated as an equivalent sphere), $\bar{v}$ and $\bar{v}_s$ are the partial specific volumes of the protein and preferentially bound solvent (H_2O), respectively, Γ' is the preferential hydration in grams of water per gram of protein, and N is Avogadro's number. For *E. coli* RNA polymerase, reported values for $\bar{v}$ and Γ' are 0.738 mL/g and 0.39, respectively (Berg & Chamberlin, 1970). Our estimates for the viscosity of TEGD at 5 °C are 1.76 cP (+0.1 M NaCl) and 1.83 cP (+1 M NaCl).

In the case of the ellipsoid, the preexponential terms (α_i) (amplitudes) depend upon the orientations of the transition moments to the symmetry axis. The rotational correlation times (ϕ_i) depend upon the diffusion constants $D_\perp$ and $D_\parallel$ for transverse and axial rotation, i.e., for motions about the short and long axes of the ellipsoid, respectively ($\phi_1 < \phi_2 < \phi_3$).

i	α_i	ϕ_i^{-1}
1	$(3/10)\sin^2\mu\sin^2\epsilon\cos 2\nu$	$4D_\parallel + 2D_\perp$
2	$(3/10)\sin 2\mu\sin 2\epsilon\cos\nu$	$D_\parallel + 5D_\perp$
3	$(2/5)P_2(\cos\mu)P_2(\cos\epsilon)$	$6D_\perp$

(7)

The polar coordinates of the two absorption transition moments (singlet–singlet and triplet–triplet) in the frame of the ellipsoid are (ϵ,0) and (μ,ν), respectively. [Angles ϵ, μ, ν, and δ are interrelated by the formula $\cos\nu = (\cos\delta - \cos\mu\cos\epsilon)/(\sin\mu\sin\epsilon)$.] For random orientation, α_1, α_2, and α_3 have the relative magnitudes 2:2:1 (Rigler & Ehrenberg, 1973). $D_\perp$ and $D_\parallel$ are analytical functions of the molecular dimensions, i.e., axes (Small & Isenberg, 1977).

The simplest model considered for the rotational relaxation of the DNA fragments is that of a rigid rod. In this case, the anisotropy decay has the same form as for the ellipsoid (the corresponding expressions for $D_\perp$ and $D_\parallel$ will be given under Discussion).

Results

Triplet Absorption Decay. Rose Bengal and eosin have similar structures and high triplet quantum yields due largely to the facilitation of intersystem crossing by the internal heavy atoms (Cherry et al., 1976). The triplet excited state of eosin has a broad absorption spectrum between 500 and 650 nm and a singlet absorption peak at 522 nm ($\epsilon = 8.3 \times 10^4$ M^{-1} cm^{-1}) (for the conjugated dye at 531 nm). Thus, the monitoring He–Ne laser line at 632.8 nm is in a region where any absorption transients are due exclusively to changes in the population of the triplet state. Rose Bengal has singlet and apparently triplet spectra similar to those of eosin since the signal amplitudes at 632.8 nm are comparable.

Figure 1 shows the isotropic decay curves for EITC and RB for both free and bound dye, together with the computer-generated exponential fits. The decay curves for both free dyes are fit well by single exponentials. Table I summarizes the computer-determined parameters. As was mentioned above, the anomalously short times seen here are due apparently to quenching effects from singlet–triplet interactions. The dyes

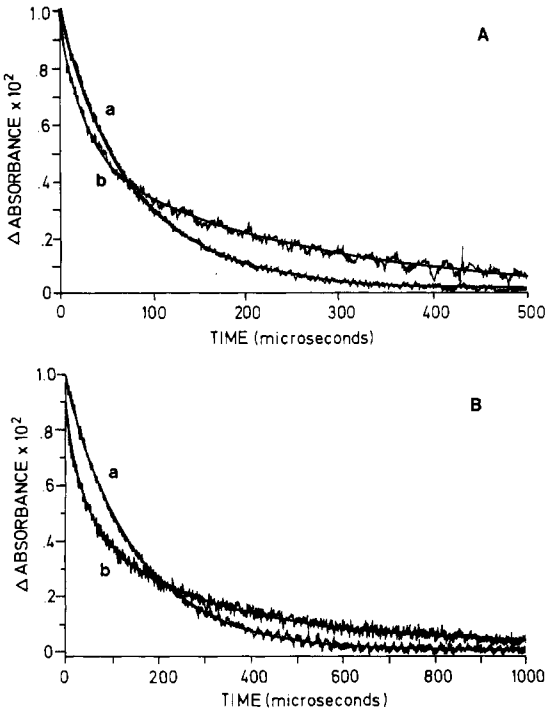

FIGURE 1: Time-resolved linear dichroism of triplet probes. (A) Rose Bengal in TEGD at 5 °C: (a) free dye; (b) dye bound to RNAP holoenzyme. The smooth lines through the data in this and other figures are the computer fits (Tables I–III). (B) Corresponding data for eosin isothiocyanate.

Table I: Triplet Lifetimes of Rose Bengal and EITC[a]

dye	free τ (μs)	bound (conjugated) to RNAP τ_1[b] (μs)	τ_2[b] (μs)
RB	91 ± 5	29 ± 2	244 ± 12
EITC	146 ± 7[c]	35 ± 2	288 ± 14

[a] χ^2 values for the analyses were 1.4–2.2. Temperature = 5 °C. [b] Amplitudes were equal within experimental error. [c] Hydrolyzed reagent in aqueous solution.

bound to protein exhibited more complex multiexponential decay kinetics probably due to perturbation of the electronic states of the dye molecule or environmental heterogeneity [see also Cherry & Schneider (1976), Austin et al. (1979), and Jovin et al. (1981)].

Stability of the Protein–Dye Complex. Our technique requires that the dye remain bound to the protein for a time much longer than the longest observed correlation time. EITC reacts so as to form a stable covalent conjugate. The noncovalent complex of RB with RNAP has a dissociation constant of 1 μM (Wu, C.-W., & Wu, 1973). A determination of the binding kinetics was required in order to define the mean lifetime of the complex. We performed stopped-flow chemical kinetic experiments by using the fluorescence enhancement of RB upon binding to RNAP (Wu, F.Y.-H., & Wu, 1973). The results indicated a k_{on} of approximately 10^8 M^{-1} s^{-1}, which yields for the dissociation rate constant a value of $\sim 10^2$ s^{-1}. Thus, the lifetime of the complex is sufficiently long ($\sim$10 ms) so as to ensure that the system remains in static equilibrium on the time scale of the anisotropy decay (10–20 μs).

Anisotropy Decay of RNAP Free in Solution. The rotational relaxation of RB–RNAP holoenzyme in TEGD + 0.1 M NaCl at 5 °C is shown in Figure 2. The decay was monoexponential under these and the other conditions summarized in Table II. At low salt concentration (0.1 M NaCl), a condition known a favor the dimeric form of the holoenzyme (Berg & Chamberlin, 1970; Shaner et al., 1982), a rotational

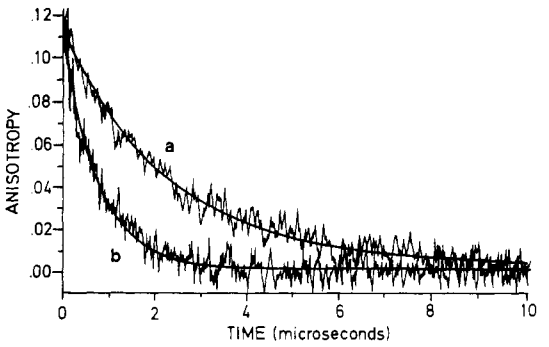

FIGURE 2: Anisotropy decay of Rose Bengal bound to RNA polymerase holoenzyme at (a) 0.1 and (b) 1 M NaCl. Temperature = 5 °C.

Table II: Rotational Relaxation of *E. coli* RNAP Holoenzyme from Triplet Probe Anisotropy

probe	[NaCl][a] (M)	ϕ (μs)	r_h[b] (nm)
RB	0.1	2.0 ± 0.5	10
RB	1.0	0.66 ± 0.05	6.9
EITC	0.1	0.65 ± 0.05	7.0

[a] In addition to standard TEGD buffer. Temperature = 5 °C. [b] Calculated from eq 6 for the equivalent hydrodynamic sphere (see text).

correlation time of 2 μs was obtained. In 1 M NaCl, the holoenzyme is monomeric (Berg & Chamberlin, 1970; Shaner et al., 1982), and the correlation time was 0.66 μs, a value similar to that previously reported from fluorescence depolarization experiments (Wu et al., 1975) but greater than the 0.44 μs predicted from eq 5 and 6. Systematic discrepancies of this magnitude are commonly observed (Cherry & Schneider, 1976; James et al., 1978; Austin et al., 1979). In the present case, deviations from a globular structure appear to be responsible. A roughly triangular flattened shape has been deduced for the monomeric holoenzyme from X-ray scattering (Meisenberger et al., 1981) and neutron scattering (Stöckel et al., 1980) measurements; eccentric shapes have also been visualized by electron microscopy (Williams, 1977). From the X-ray data obtained at 5 °C, values of 790 nm^3 and 7.2–7.4 nm were deduced for the molecular volume and radius of gyration, respectively. We calculated 6.9 nm for the radius of the equivalent hydrodynamic sphere from our data and eq 6, and 7.6 nm from the reported translational diffusion constant (2.0×10^{-7} cm^2 s^{-1}; Shaner et al., 1982). We can reconcile the measured rotational correlation time with the known molecular weight by assuming that RNAP has the shape of an oblate ellipsoid (for which the decay of anisotropy is essentially monoexponential: $\phi_1 \cong \phi_2 \cong \phi_3$; Small & Isenberg, 1977). Axial ratios of 2, 3, and 4 would correspond to rotational correlation times at 5 °C of 0.53, 0.70, and 0.84 μs, respectively. Thus, an oblate ellipsoid with an axial ratio of about 3 fits the data and also offers a reasonable approximation to the geometry derived from the X-ray scattering studies. Such a flattened disc model may be even more appropriate in the case of the holoenzyme dimer for which a radius of gyration of 8 nm has been reported (Heumann et al., 1982) and for which we obtained a Stokes radius (equivalent hydrodynamic sphere) of 10 nm (Table II, eq 5 and 6).

Except in 1 M NaCl, preparations of core enzyme showed a multiexponential mode of anisotropy decay, a finding consistent with the concentration-dependent multimeric aggregation observed for this species in scattering (Heumann et al., 1982) and hydrodynamic (Shaner et al., 1982) studies. It is interesting that the holoenzyme derivatized with EITC did not

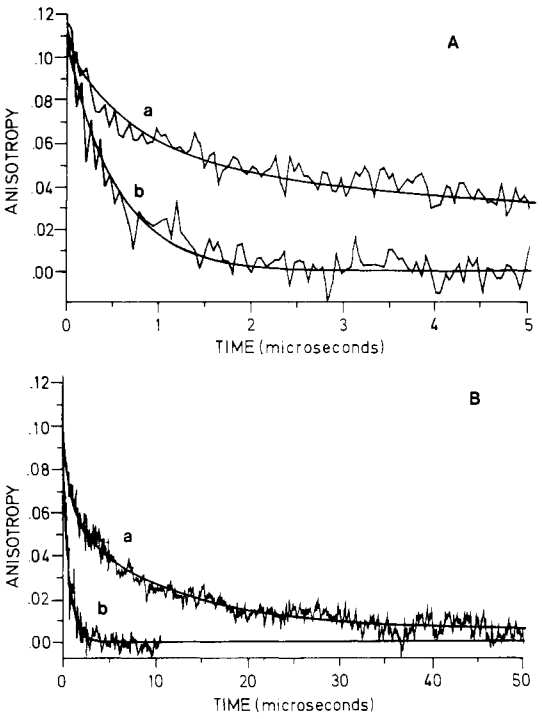

FIGURE 3: Anisotropy decay of Rose Bengal–RNAP holoenzyme bound to poly[d(A-T)]. (A) Time range 0–5 μs: (a) 0.1 M NaCl; (b) 1 M NaCl. (B) Time range 0–50 μs.

Table III: Rotational Relaxation of *E. coli* RNAP Holoenzyme Bound to DNA[a]

conditions	[NaCl][b] (M)	fast component		slow component	
		α_f	ϕ_f (μs)	α_s	ϕ_s (μs)
RB-enzyme + poly[d(A-T)]	0.1	0.06	0.7 ± 0.1	0.06	11 ± 5
RB-enzyme + poly[d(A-T)]	1.0	0.13	0.5 ± 0.1		
RB-enzyme + calf thymus DNA	0.1	0.07	0.5 ± 0.1	0.07	14 ± 5
eosin-enzyme + poly[d(A-T)]	0.1	0.09	0.5 ± 0.1	0.09	14 ± 5

[a] All amplitudes are ±0.01. Temperature = 5 °C. [b] In addition to standard TEGD buffer.

appear to dimerize in low salt (Table II) as if the dye interferes with the quaternary interactions required for association; the enzymatic activity, however, was preserved.

From the r_{in} value of about 0.12 (Figure 2) and eq 4, we calculate that the singlet–singlet and triplet–triplet transition moments are separated by an angle $\delta < 43°$.

Anisotropy Decay of RNAP Bound to DNA. "Typical" decay curves for RNAP bound to poly[d(A-T)] at 0.1 and 1.0 M NaCl are shown in Figure 3. The latter sections will discuss the effects of varying parameters, while here we restrict ourselves to the main features of the decay curves and define our terminology.

The most striking aspect of the curves is that the residual anisotropy at long time (50 μs) is zero. Thus, there is no hindered rotation beyond the limits of experimental resolution. The next major point is the multiexponential nature of the decay curves obtained in 0.1 M NaCl. Table III shows that at least two components were required in order to fit the data with rotational correlation times at 5 °C of 0.5 ± 0.1 and 14 ± 5 μs. We denote the ratio of the fast component to the total anisotropy amplitude as R:

$$R = A_{fast}/(A_{fast} + A_{slow}) \quad (8)$$

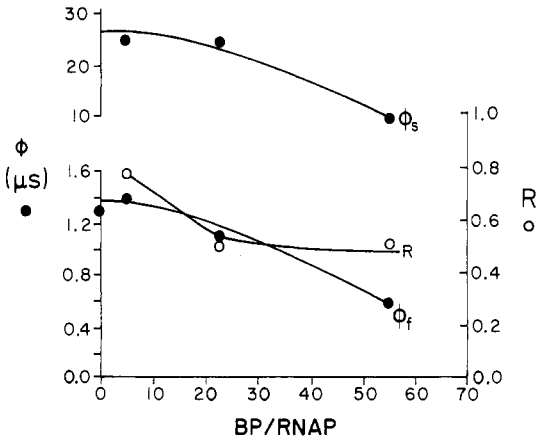

FIGURE 4: Dependence of the rotational correlation times and the relative amplitudes on the ratio of DNA concentration (base pairs) to RNA polymerase concentration (BP/RNAP). Data for RB–RNAP + poly[d(A-T)] in 0.1 M NaCl and 5 °C. The left-hand axis depicts the rotational correlation times (fast and slow), and the right-hand axis is the amplitude ratio $R = A_f/(A_f + A_s)$ (eq 8 in the text). Lines drawn through the points are by hand and serve as a guide. No further changes were seen for BP/RNAP >55 (data not shown).

A submicrosecond uniphasic rotational relaxation was seen in the presence of DNA but at high salt concentration (1 M NaCl, Figure 3), a condition under which holoenzyme monomerizes (see above) and does not bind to DNA (Smith et al., 1976; Revzin & Woychik, 1981; Shaner et al., 1983). Attempts to use core RNAP at 5 μM concentration invariably resulted in turbid suspensions upon addition of DNA, an effect not observed in the case of the holoenzyme.

The majority of experiments were performed with the RB–enzyme. The behavior of the protein labeled with EITC was essentially the same.

Anisotropy as a Function of DNA/RNAP Ratio. Titration of holo-RNAP solution with DNA should generate decay curves demonstrating the heterogeneous superposed rotational properties of free and bound enzyme. To test this, we added increasing quantities of poly[d(A-T)] (chain length 700–800 bp) to a 6 μM solution of RB–RNAP (Figure 4). The quantity R defined above decreased with increasing ratio of DNA base pairs to polymerase and reached the limiting value of 0.5 characteristic for enzyme saturated with DNA (Table III) at a DNA (base pair)/enzyme ratio of 20. The rotational correlation times also shortened with addition of DNA and achieved final values by a DNA/enzyme ratio of 55. We attribute the faster rotational relaxation to the combined effects of monomerization of the enzyme upon DNA binding and the reduction in mass per unit length of DNA (Pörschke et al., 1982).

Anisotropy Decay as a Function of DNA Composition. Much of our data was obtained by using poly[d(A-T)] to form binary complexes with RNAP. However, this synthetic polynucleotide has physical and functional properties quite distinct from those of natural DNA sequences (see the introduction). For example, the self-complementary sequence potentiates the formation of hairpin helices (Baldwin, 1971). Furthermore, poly[d(A-T)] can adopt two conformations in solution depending upon the ionic environment and cationic ligands (Patel et al., 1981). One of them appears to be a right-handed B-DNA structure with a dinucleotide repeat (Viswamitra et al., 1982; Eckstein & Jovin, 1983). The rotational relaxations observed in binary complexes of RNAP with poly[d(A-T)] and calf thymus DNA were nonetheless indistinguishable at our level of experimental accuracy (Table III).

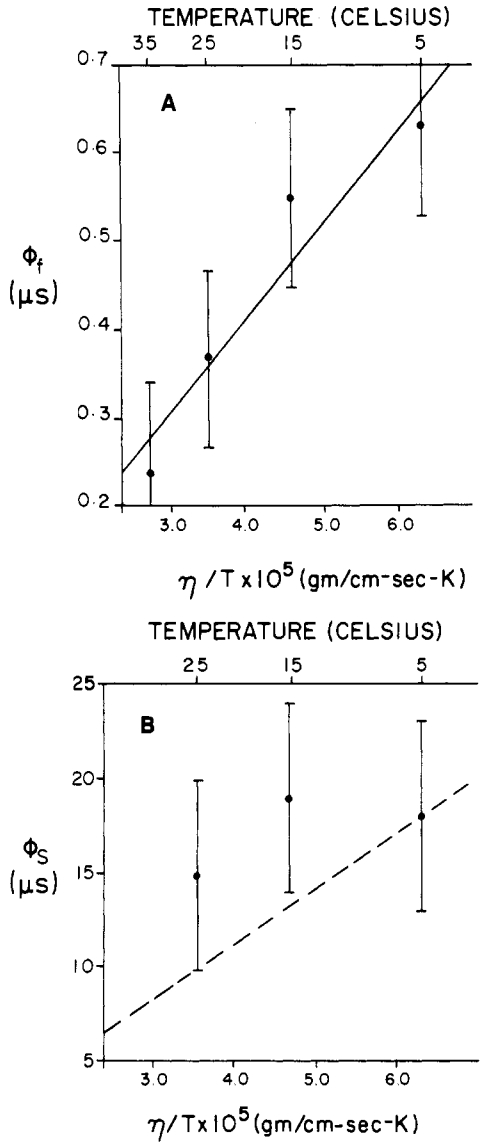

FIGURE 5: Dependence of the rotational correlation times on the ratio η/T. Data for RB–RNAP + poly[d(A-T)] in 0.1 M NaCl. (A) Fast component, ϕ_f. The straight line is a least-squares fit by using eq 5 and 6 and corresponds to a sphere with a hydrodynamic radius of 6.9 nm. (B) Slow component, ϕ_s. The dashed line is calculated for a rigid rod (ϕ_3, eq 7 and 9) of length 85 nm. The errors are greater than those in (A) due to the small relative amplitude of the slow component.

Anisotropy Decay as a Function of Temperature. If the anisotropy decay curves represent rotational reorientation in a viscous medium defined by the bulk solvent viscosity η, the correlation times should be proportional to η/T (as the temperature is raised). The fast component as well as the single correlation time measured with free RB–holoenzyme exhibited the expected behavior in conformity with eq 5, 9, and 10 (Figure 5A). The long correlation time (Figure 5B) gave a less adequate fit, but the errors associated with the small amplitudes at the higher temperatures are considerable.

The dependence of R (eq 2) on temperature is shown in Figure 6. It can be seen that the relative magnitude of the fast component increased with temperature (the total initial anisotropy at 50 ns remained constant at 0.12–0.14). Simple theories for DNA motion predict that R should be temperature independent (see Discussion).

Anisotropy Decay as a Function of DNA Chain Length. The rotational properties of RB–enzyme/DNA binary complexes were studied as a function of DNA chain length by

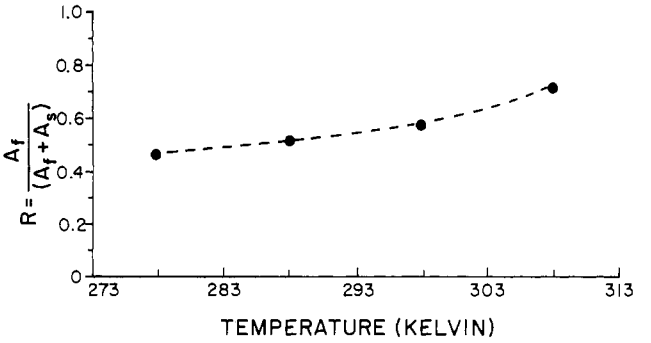

FIGURE 6: Fractional amplitude of the fast component (R) as a function of temperature. Data as in Figure 5.

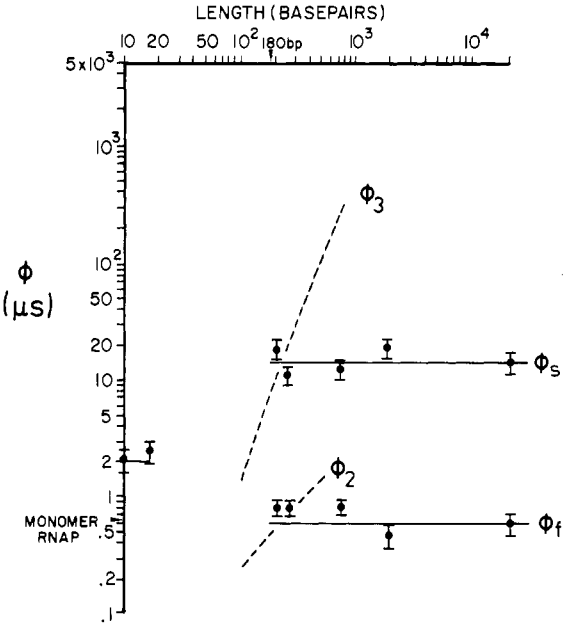

FIGURE 7: Rotational correlation times as a function of DNA fragment length. Data for RB–RNAP holoenzyme + poly[d(A-T)] in 0.1 M NaCl at 5 °C. The dashed lines depict the two longest correlation times calculated for a rigid rod (eq 3, 7, 9, and 10). The point marked "monomer RNAP" refers to the value in 1 M NaCl (Table II). For DNA fragments of length 10 and 15 bp, the decay was monoexponential.

using defined poly[d(A-T)] fragments (Figure 7). The total DNA and RNAP concentrations were held approximately constant at 1 mM (base pairs) and 4 μM, respectively. Neither the long (nominal 14 μs) nor the short correlation times varied above a chain length of 190, i.e., approximately one persistence length (see below). However, the oligonucleotide $(dAT)_{10}$ did not appreciably influence the anisotropy decay of the labeled enzyme, but the extent of binding was not assessed by other means.

Discussion

The triplet probes and transient dichroism techniques employed in this study clearly resolve the rotational dynamics of RNA polymerase in the free state as well as bound to DNA. The isotropic rotational correlation times measured via bound Rose Bengal of holoenzyme in the dimeric (2.0 μs, 0.1 M NaCl) and monomeric (0.66 μs, 1 M NaCl) states at 5 °C agree well with other available physical and hydrodynamic data if one assumes the shape of an oblate ellipsoid.

The rotational diffusion of RNA polymerase changes dramatically upon binding to DNA and provides direct evidence for a complex chracterized by considerable structural and temporal (lifetime >50 μs) stability. Two correlation times (typically 0.6 and 14 μs) describe the decay of linear dichroism

of complexes formed at 5 °C with either poly[d(A-T)] or calf thymus DNA. These values are shorter and longer, respectively, than any observed with the free holoenzyme (in 0.1 M NaCl) and suggest that the protein monomerizes upon binding to the DNA (in accordance with expectation) and that the end over end tumbling, possibly the spinning motion as well, of the binary complex is determined largely by the hydrodynamic properties of the DNA. We now consider quantitative arguments in support of this interpretation.

The rotational diffusion of DNA can be described by different formalisms depending upon the length of the double helix and environmental conditions (temperature, ionic strength). According to the representation of DNA as a uniformly elastic rod, the measure of bending rigidity is given by the persistence length, a configurational parameter for which the currently accepted value is about 50 nm or approximately 150 base pairs (Hagerman, 1981). The hydrodynamic properties of DNA molecules smaller than the persistence length are fairly well described by the formulas applicable to rigid rods [Hogan et al., 1978; Elias & Eden, 1981; for deviations, see Hagerman (1981) and Early et al. (1981)]. Wormlike chain models apply for longer molecules (Hagerman & Zimm, 1981; Diekmann et al., 1982). More recently, the theories have been extended to account for twisting deformations and other ligand-associated internal motions (Barkley & Zimm, 1979; Schurr, 1982) and subjected to experimental test by a number of techniques [picosecond fluorescence depolarization (Millar et al., 1980), proton NMR (Early et al., 1981), and triplet-state depolarization (Hogan et al., 1982; Wang et al., 1982)].

The long rotational correlation time we observed for enzyme–DNA complexes was independent of DNA size above the persistence length limit. This finding presumably derives from the fact that the triplet probe residues on the enzyme, thereby restricting the optical observation to the *segmental* diffusion of the binding site and the DNA regions in immediate contiguity [for discussions of segmental diffusion, see Berg (1979), Wegener (1982), and Schurr (1982)]. As an initial approximation, we apply the rigid rod formalism to the DNA component in the form of the expressions for the transverse diffusion constant $D_\perp$ [see Broersma in Chen et al. (1980)] and axial diffusion constant $D_\parallel$ [de la Torre & Bloomfield, 1981; the correct form of their eq 74 is given in Tirado & de la Torre (1980)] which correspond to the end over end tumbling and the spinning motions, respectively.

$$D_\perp = [3kT/(\pi\eta L^3)]\{\ln p - 0.76 - 7.5[1/(\ln 2p) - 0.27]^2\} \quad (9)$$

$$D_\parallel = [kT/(0.96\pi\eta L d^2)]/[1 + 0.677/p - 0.183/p^2] \quad (10)$$

L and d are the length and diameter of the rod, respectively, and p is the axial ratio L/d.

Introducing the values $L = 50$ nm and $d = 2.6$ nm into eq 9 and 10 leads to $D_\perp = 3.66 \times 10^4$ s^{-1} and $D_\parallel = 2.07 \times 10^6$ s^{-1} at 5 °C. The corresponding rotational correlation times (eq 7) are 0.12, 0.44, and 4.6 μs. For $L = 80$ nm, $D_\perp$ and $D_\parallel$ are 1.09×10^4 and 1.31×10^6 s^{-1}, respectively, leading to correlation times of 0.19, 0.73, and 15.3 μs. These values (except for the fastest component) are remarkably similar to those actually measured for the enzyme–DNA complex. We now consider the simplest possible model for the latter, namely that of a globular protein (sphere) disposed symmetrically about the DNA axis such that the rotational friction coefficient of the ensemble f^* is given by the sum of the individual coefficients. Since in general $f = kT/D$, the resultant diffusion constants are the harmonic means.

$$D_\perp^* = 1/[1/D_{\perp,\mathrm{RNAP}} + 1/D_{\perp,\mathrm{DNA}}] \quad (11a)$$

$$D_\parallel^* = 1/[1/D_{\parallel,\mathrm{RNAP}} + 1/D_{\parallel,\mathrm{DNA}}] \quad (11b)$$

From a ϕ of 0.66 μs, $D_{\perp,\mathrm{RNAP}} = D_{\parallel,\mathrm{RNAP}} = 2.5 \times 10^5$ s^{-1}. Calculation of $D_\perp^*$ and $D_\parallel^*$ by using values appropriate for $L = 50$ and $L = 80$ and introduction into eq 11 lead to estimates of the rotational correlation times of 1.0, 2.6, and 5.2 μs ($L = 50$) and 1.2, 3.8, and 15.9 μs ($L = 80$). Furthermore, for a random orientation of the transition moments relative to the rotation axis (the expectation in the case of eosin conjugates), the relative amplitudes should obey a 2:2:1 relationship. Clearly, the observed decay of anisotropy does not follow this predicted behavior, and we conclude that the simple model of a rigid complex and a spherical protein does not apply. At least four alternative possibilities merit consideration and supply the basis for further work.

(*1*) *Asymmetry and/or Conformational Change in RNAP.* The protein is asymmetrically disposed (e.g., long axis aligned parallel to the DNA helix) and/or undergoes a conformational change upon binding to the DNA (see the introduction). Particularly if accompanied by a certain loss of structural rigidity, this process would lead to an increase in the effective $D_\parallel$ by a factor which if greater than approximately 6 would lead to agreement with the two longer correlation times predicted for $L = 80$ for DNA alone (see above) and the actual measurements (the fastest being beyond the time resolution of the experiments). In effect, the protein would be functioning as a reporter group, operationally similar to a small intercalating drug (Hogan et al., 1982), devoid of significant hydrodynamic drag in the bound state.

(*2*) *Alteration of DNA Structure.* The bound enzyme modifies the DNA structure locally, e.g., by denaturation [see the introduction; also see Gamper & Hearst (1982)], and thus uncouples to a certain degree its rotational relaxation from that of the DNA. The temperature-dependent relative amplitudes might be reflections of such a process which would influence both the torsional and bending rigidity of the DNA as sensed by the protein. The formalism for treating swivel-jointed or hinged structures (e.g., rods) is available (Wegener, 1980, 1982) but has yet to be applied rigorously to the specific situation represented in this work. One effect would be to reduce the longest correlation time associated with tumbling by up to a factor of 4–5 (Wegener, 1980). As suggested by the experimental results (e.g., ϕ_f in Figure 5 and the amplitude trend in Figure 6), the axial relaxation exhibited by the protein could approach that which it experiences in the free state, depending upon the mechanical properties of the protein–DNA junction. Theoretical features requiring further consideration are the relationship of the hydrodynamic center of rotation to the center of mass of the protein and the degree of corresponding rotational–translational coupling (de la Torre & Bloomfield, 1981; Wegener, 1980, 1982).

(*3*) *Enzyme Translocation (Sliding, Rotation).* The nonspecific complexes described here are of interest because they presumably represent intermediates in the overall process by which regulatory proteins interact with DNA and locate physiologically relevant targets (von Hippel & Bear, 1983; Fried & Crothers, 1983), e.g., by one-dimensional diffusion along the DNA axis. This sliding mechanism has been treated extensively by theory [e.g., see Berg & Ehrenberg (1982) and Berg et al. (1981)] and applied to experimental data. For the *lac* repressor, a one-dimensional diffusion constant of about 10^{-9} cm^2 s^{-1} has been estimated (Barkley, 1981; Winter et al., 1981), a value which corresponds to a net displacement or scanning of about 3 bp in 10 μs. A corresponding number for RNAP has neither been determined experimentally nor been

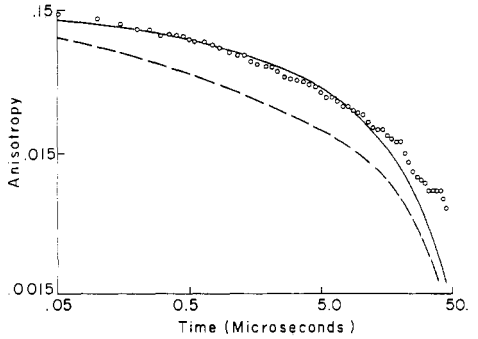

FIGURE 8: Anisotropy decay data for the RNAP–DNA complex fit with the torsionally flexible filament model for DNA. Data from Figure 3 (0.1 M NaCl) plotted on log–log axes (O). The solid line is from the theory of J. M. Schurr using a rotational friction coefficient of 7.8×10^{-23} erg s. The dashed line simulates the anisotropy decay of DNA by using a rotational friction coefficient of 10^{-23} erg s. The calculations assumed a random orientation of the triplet probe, an angle δ (eq 4) of 35°, a length of 600 bp, and a bending function with a single exponential time constant of 14 μs.

estimated. Its magnitude would depend upon the nature of the sliding mechanism(s) (Berg et al., 1982; von Hippel & Bear, 1983) and whether the enzyme must rotate about the DNA helix axis in order to maintain stereospecific interactions during recognition and/or active translocation (Somogyi et al., 1977; Schurr, 1979; Dennis & Sylvester, 1981). Using a translation–rotation coupled hydrodynamic model (Schurr, 1979), one would predict that the diffusion constant for RNA polymerase would be about 3 times lower than that for *lac* repressor, leading to an effective scanning rate of about 1–2 bp (or 10–20% of a turn) in 10 μs. Such a motion would not have contributed appreciably to the observed rotational depolarization. However, a faster scanning rate would be detected.

(*4*) *Twisting and Bending Motions of the DNA.* DNA is no longer regarded as a rigid rod but an elastic structure exhibiting torsional (twisting) deformations. The bound enzyme would sense these torsional fluctuations and thus undergo a faster more "local" relaxation about the long axis of the DNA, the tumbling motion remaining approximately the same. A companion paper to this one has explored the anisotropy decay of DNA molecules alone [Hogan et al., 1982; see also Wang et al. (1982) and Millar et al. (1980)]. J. M. Schurr and co-workers have recently modified the anisotropy decay function in order to account for an elastic rod with torsional flexibility and have incorporated provisions for empirical bending motions [personal communication; see also Barkley & Zimm (1979) and Schurr (1982)]. The resultant expression has the same form (three terms, same amplitude factors) as eq 3 and 7; however, the time-dependent functions are no longer simple exponentials but rather products of functions depicting the transverse (i = 1–3) and axial (i = 1, 2) rotational reorientations. Using this formalism, we performed simulations of anisotropy decay curves for DNA alone and for DNA loaded with two RNAP polymerase molecules per 60 nm (the average value for most of our experiments) (Figure 8). The fits are satisfactory and compatible with the notion that RNA polymerase does not alter the torsional rigidity of the DNA, at least not to the extent envisioned under (2) above. The temperature dependence of this model has yet to be explored in order to see if it accounts for the data in Figure 6.

The experiments reported here represent the first attempts to define the properties of RNA polymerase–DNA interactions by using time-resolved measurements in the microsecond to millisecond range. They are currently being extended to studies of defined promoter-containing fragments and to RNA polymerase under a state of active transcription. Clearly, other DNA-binding proteins can be investigated in a similar manner.

Acknowledgments

We thank Manfred Eigen and express indebtedness to the late Hermann Träuble for their generosity in support of this work. R.H.A. thanks M. Hogan, J. Hearst, S. Hershkowitz, and C. Monitto for good advice and S. Chan for encouragement and support. J. M. Schurr was particularly patient in explaining his work and generous in sharing his results prior to publication.

Registry No. RNA polymerase, 9014-24-8; RB, 11121-48-5; EITC, 60520-47-0; poly[d(A-T)], 26966-61-0.

References

Austin, R. H., Chan, S. S., & Jovin, T. M. (1979) *Proc. Natl. Acad. Sci. U.S.A. 76*, 5650–5654.
Baldwin, R. L. (1971) *Acc. Chem. Res. 4*, 265–272.
Barkley, M. D. (1981) *Biochemistry 20*, 3833–3842.
Barkley, M. D., & Zimm, B. H. (1979) *J. Chem. Phys. 70*, 2991–3007.
Berg, D., & Chamberlin, M. (1970) *Biochemistry 9*, 5055–5064.
Berg, D., Barrett, K., & Chamberlin, M. (1971) *Methods Enzymol. 21*, 506–519.
Berg, O. G. (1979) *Biopolymers 18*, 2861–2874.
Berg, O. G., & Ehrenberg, M. (1982) *Biophys. Chem. 15*, 41–51.
Berg, O. G., Winter, R. B., & von Hippel, P. H. (1981) *Biochemistry 20*, 6929–6948.
Burgess, R. R. (1976) in *RNA Polymerase* (Losick, R., & Chamberlin, M., Eds.) p 69, Cold Spring Harbor Laboratory, Cold Spring Harbor, NY.
Chen, F. C., Koopmans, G., Wiseman, R. L., Day, L. A., & Swinney, H. L. (1980) *Biochemistry 19*, 1373–1376.
Cherry, R. J. (1978) *Methods Enzymol. 54*, 47–61.
Cherry, R. J., & Schneider, G. (1976) *Biochemistry 15*, 3657–3661.
Cherry, R. J., Cogoli, A., Oppliger, M., Schneider, G., & Semenza, G. (1976) *Biochemistry 15*, 3653–3656.
de Haseth, P. L., Lohman, T. M., Burgess, R. R., & Record, M. T., Jr. (1978) *Biochemistry 17*, 1612–1622.
de la Torre, J. G., & Bloomfield, V. A. (1981) *Q. Rev. Biophys. 14*, 81–139.
Dennis, D., & Sylvester, J. E. (1981) *FEBS Lett. 124*, 135–139.
Diekmann, S., Hillen, W., Morgeneyer, B., Wells, R. D., & Pörschke, D. (1982) *Biophys. Chem. 15*, 263–270.
Early, T. A., Kearns, D. R., Hillen, W., & Wells, R. D. (1981) *Biochemistry 20*, 3764–3769.
Eckstein, F., & Jovin, T. M. (1983) *Biochemistry* (in press).
Elias, J. G., & Eden, D. (1981) *Biopolymers 20*, 2369–2380.
Fried, M. G., & Crothers, D. M. (1983) *Cold Spring Harbor Symp. Quant. Biol.* (in press).
Gamper, H. B., & Hearst, J. E. (1982) *Cell (Cambridge, Mass.) 29*, 81–90.
Hagerman, P. J. (1981) *Biopolymers 20*, 1503–1535.
Hagerman, P. J., & Zimm, B. H. (1981) *Biopolymers 20*, 1481–1502.
Heumann, H., Meisenberger, O., & Pilz, I. (1982) *FEBS Lett. 138*, 273–276.
Hogan, M., Dattagupta, N., & Crothers, D. M. (1978) *Proc. Natl. Acad. Sci. U.S.A. 75*, 195–199.
Hogan, M., Wang, J., Austin, R. H., Monitto, C. L., & Hershkowitz, S. (1982) *Proc. Natl. Acad. Sci. U.S.A. 79*, 3518–3522.

James, T. L., Matson, G. B., & Kuntz, I. D. (1978) *J. Am. Chem. Soc. 100*, 3590–3594.
Jovin, T. M., Bartholdi, M., Vaz, W. L. C., & Austin, R. H. (1981) *Ann. N.Y. Acad. Sci. 366*, 176–196.
Kabsch, W., Sander, C., & Trifonov, E. N. (1982) *Nucleic Acids Res.*, 1097–1104.
Kadesch, T. R., Robley, C. W., & Chamberlin, M. J. (1980) *J. Mol. Biol. 136*, 65–78.
Krakow, J. S., & von der Helm, K. (1970) *Cold Spring Harbor Symp. Quant. Biol. 35*, 73–83.
Kumar, S. A. (1981) *Prog. Biophys. Mol. Biol. 38*, 165–210.
Levine, B. J., Orphanos, P. D., Fischmann, B. S., & Beychok, S. (1980) *Biochemistry 19*, 4808–4814.
Lohman, T. M., de Haseth, P. L., & Record, M. T., Jr. (1980) *Biochemistry 19*, 3522–5230.
McClure, W. R. (1980) *Proc. Natl. Acad. Sci. U.S.A. 77*, 5634–5638.
Meisenberger, O., Heumann, H., & Pilz, I. (1981) *FEBS Lett. 123*, 22–24.
Melançon, P., Burgess, R. R., & Record, M. T., Jr. (1982) *Biochemistry 21*, 4318–4331.
Melnikova, A. F., Beabealashvilli, R., & Mirzabekov, A. D. (1978) *Eur. J. Biochem. 84*, 301–309.
Millar, D. P., Robbins, R. J., & Zewail, A. H. (1980) *Proc. Natl. Acad. Sci. U.S.A. 77*, 5593–5597.
Parks, C. S., Hillel, A., & Wu, C.-W. (1980) *Nucleic Acids Res. 23*, 5895–5912.
Patel, D. J., Kozlowski, S. A., Suggs, J. W., & Cox, S. D. (1981) *Proc. Natl. Acad. Sci. U.S.A. 78*, 4063–4067.
Pörschke, D., Geisler, N., & Hillen, W. (1982) *Nucleic Acids Res. 10*, 3791–3802.
Reisbig, R. R., Woody, A.-Y. M., & Woody, R. W. (1979) *J. Biol. Chem. 254*, 11208–11217.
Reisbig, R. R., Woody, A.-Y. M., & Woody, R. W. (1981) *Biochim. Biophys. Acta 652*, 294–302.
Revzin, A., & Woychik, R. P. (1981) *Biochemistry 20*, 250–256.
Rigler, R., & Ehrenberg, M. (1973) *Q. Rev. Biophys. 6*, 139–199.
Schurr, J. M. (1979) *Biophys. Chem. 9*, 413–414.
Schurr, J. M. (1982) *Chem. Phys. 65*, 417–424.
Shaner, S. L., Piatt, D. M., Wensley, C. G., Yu, H., Burgess, R. R., & Record, M. T., Jr. (1982) *Biochemistry 21*, 5539–5551.
Shaner, S. L., Melançon, P., Lee, K. S., Burgess, R. R., & Record, M. T., Jr. (1983) *Cold Spring Harbor Symp. Quant. Biol.* (in press).
Shimamoto, N., & Wu, C.-W. (1980) *Biochemistry 19*, 842–848.
Siebenlist, U., Simpson, R. B., & Gilbert, W. (1980) *Cell (Cambridge, Mass.) 20*, 269–281.
Small, E. W., & Isenberg, I. (1977) *Biopolymers 16*, 1907–1928.
Smith, D. A., Martinez, A. M., Ratcliff, R. L., & Williams, D. L. (1967) *Biochemistry 6*, 3057–3064.
Somogyi, B., Trőn, L., & Damjanovich, S. (1977) *J. Theor. Biol. 67*, 175–180.
Stender, W. (1979) *FEBS Lett. 103*, 57–60.
Stöckel, P., May, R., Strell, I., Cejka, Z., Hoppe, W., Heumann, H., Zillig, W., & Crespi, H. (1980) *Eur. J. Biochem. 112*, 411–417.
Strauss, H. S., Burgess, R. R., & Record, T. M., Jr. (1980) *Biochemistry 19*, 3496–3504.
Studier, F. W. (1965) *J. Mol. Biol. 11*, 373–390.
Tirado, M. M., & de la Torre, J. G. (1980) *J. Chem. Phys. 73*, 1986–1993.
Viswamitra, M. A., Shakked, Z., Jones, P. G., Sheldrick, G. M., Salisbury, S. A., & Kennard O. (1982) *Biopolymers 21*, 513–533.
von Hippel, P. H., & Bear, D. G. (1983) *Mobility and Recognition in Cell Biology* (Sund, H., & Veeger, C., Eds.) pp 291–316, Walter de Gruyter, Berlin.
Wang, J., Hogan, M., & Austin, R. H. (1982) *Proc. Natl. Acad. Sci. U.S.A. 79*, 5896–5900.
Wegener, W. A. (1980) *Biopolymers 19*, 1899–1908.
Wegener, W. A. (1982) *Biopolymers 21*, 1049–1080.
Williams, R. C. (1977) *Proc. Natl. Acad. Sci. U.S.A. 74*, 2311–2315.
Winter, R. B., Berg, O. G., & von Hippel, P. H. (1981) *Biochemistry 20*, 6961–6977.
Wu, C.-W., & Wu, F. Y.-H. (1973) *Biochemistry 12*, 4349–4355.
Wu, C.-W., Yarbrough, L. R., Hillel, Z., & Wu, F. Y.-H. (1975) *Proc. Natl. Acad. Sci. U.S.A. 72*, 3019–3023.
Wu, F. Y.-H., & Wu, C.-W. (1973) *Biochemistry 12*, 4343–4348.